

FRICION FACTOR IN HIGH PRESSURE NATURAL GAS PIPELINES FROM ROUGHNESS MEASUREMENTS

DETERMINATION DU COEFFICIENT DE FRICTION DANS DES CONDUITES A HAUTE PRESSION A PARTIR DE LA RUGOSITE

E. Sletfjerd¹
J. S. Gudmundsson

Department of Petroleum Engineering and Applied Geophysics
Norwegian University of Science and Technology, Norway

ABSTRACT

Pressure drop experiments on natural gas flow at 80 to 120 bar pressure and high Reynolds number were carried out for pipes with smooth to rough surfaces. The roughness was measured with an accurate stylus instrument and analyzed using fractal methods. Using a similar approach to that of Nikuradse, the measured friction factor was correlated with the measured roughness values. Taking the value of the relative roughness and dividing it by the slope of the power spectrum of the measured roughness, a greatly improved fit with the measured friction factor was obtained. Indeed, a new friction factor correlation was obtained, but now formulated in terms of direct measurement of roughness.

RESUME

Des expériences ont été menées sur les chutes de pression dans un écoulement de gas naturel dans des conduites de rugosité variable, avec une pression comprise entre 80 et 120 bar et des nombres de Reynolds élevés. La rugosité a été mesurée avec précision par un instrument à stylet et analysée par des méthodes fractales. Suivant une approche semblable à celle de Nikuradse, les mesures du coefficient de friction ont été corrélées avec celles de la rugosité, avec un très bon accord. En prenant la valeur de la rugosité relative et en la divisant par la pente du spectre en fréquence de la rugosité mesurée, il a été obtenue une bien meilleure correspondance avec les coefficients de friction mesurés. En fait, une nouvelle expression pour le coefficient de friction a été obtenue, mais exprimée directement à partir de la mesure de la rugosité.

¹ Present address: Statoil's Research Center, 7005 Trondheim, Norway, esle@statoil.com

INTRODUCTION

High Reynolds-number flow in pipes has received renewed interest in recent years. Experimental results [1] and theoretical work [2] have questioned the validity of the scaling laws for the wall layer at high Reynolds number. The reported studies have focused on flow over smooth surfaces. In industrial applications, however, high Reynolds number flow normally leads to significant effects of wall roughness on velocity profiles and friction factors due to the small length scales involved.

Flow in offshore gas pipelines is characterized by high Reynolds numbers, typically 1×10^7 , due to the low viscosity and the relative high density of natural gas at typical operating pressures (100-180 bar). At such Reynolds numbers the classical Colebrook-White friction factor correlation [3] predicts that minute irregularities (in the order of $1 \mu\text{m}$) on the pipe wall will have a significant effect on the friction factor. Similar problems are encountered in flow past merchant ships where viscous drag dominates the resistance and the wall roughness may be a dominating factor [4].

The main reference on flow in rough pipes is still the Nikuradse work [5] in sand-grain roughened pipes. In this work Nikuradse reached a Reynolds number of 1×10^6 as maximum, one decade lower than what is typically encountered in offshore gas pipelines. The need for experimental data on flow over rough walls at high Reynolds number was pointed out by Patel [6] in a recent review paper.

This paper presents experimental results from high Reynolds number flow experiments in 8 pipes of varying wall roughness. The wall roughness was varied by mixing glass beads in the epoxy coating applied on the walls of the test pipes. The resulting wall roughness was homogenous and the asperity height was governed by the size of the glass beads in the coating. Further details are given by Sletfjerding [7].

FRICITION FACTOR CORRELATIONS

In horizontal pipe flow at moderate velocities the main cause of energy loss is the friction between the pipe wall and the moving fluid. The pressure loss due to wall friction is expressed in terms of the friction factor

$$f = \tau_w / \frac{1}{8} \rho \bar{U}^2 \quad \text{Equation 1}$$

From the one-dimensional momentum equation (Equation 2) for a horizontal pipe, the friction term dominates the pressure drop when the acceleration term is small.

$$\frac{dP}{dx} + \rho g \sin(\alpha) + \frac{f}{D} \frac{1}{2} \rho \bar{U}^2 + \frac{d(\rho \bar{U}^2)}{dx} = 0 \quad \text{Equation 2}$$

Most friction factor correlations used in industry are semi-empirical models based on turbulent boundary layer theory. The main reference for friction factors in pipes has been the work of Nikuradse [5, 8] on flow in smooth and sand roughened pipes, where friction factor relations for smooth pipes (Equation 3) and rough pipes (Equation 4) were presented. The smooth pipe law (Equation 3) was originally presented by Prandtl and the rough pipe relation (Equation 4) by Von Karman. However, the constants in both relations were adjusted by Nikuradse [5, 8] to fit his experimental data.

$$\sqrt{\frac{1}{f}} = 2.0 \log(\text{Re} \sqrt{f}) - 0.8 = 2.0 \log\left(\frac{\text{Re} \sqrt{f}}{2.51}\right) \quad \text{Equation 3}$$

$$\sqrt{1/f} = 2 \log\left(\frac{r}{k_s}\right) + 1.74 = 2 \log\left(7.41 \frac{r}{k_s}\right) \quad \text{Equation 4}$$

Nikuradse showed that for low Reynolds numbers (Re) the friction factor was a function of Re only, then at sufficiently high Re the friction factor became a function of the wall roughness only. The first case was called hydraulical smooth flow and the latter was called rough flow. Colebrook [3] presented additional experimental results and developed a correlation for the friction factor (Equation 5) valid also in the transitional regime between the smooth and rough flow.

$$\sqrt{1/f} = -2 \log\left(\frac{2.51}{\text{Re} \sqrt{f}} + \frac{k_s}{3.7D}\right) \quad \text{Equation 5}$$

The so-called Colebrook-White equation has been extensively used since it was presented. However, the implicit character of the correlation has created a need for a simpler explicit correlation. Many such correlations have been presented and one is the Haaland equation [9].

$$\sqrt{1/f} = -\frac{1.8}{n} \log\left[\left(\frac{6.9}{\text{Re}}\right)^n + \left(\frac{k_s}{3.75D}\right)^{1.11n}\right] \quad \text{Equation 6}$$

With $n=1$, the equation is a good approximation to the Colebrook-White equation with a gradual transition between smooth and rough flow. Haaland claimed that this equation is especially suited for gas pipelines if $n=3$, giving a more abrupt transition between smooth and rough flow. Most of the explicit friction factor relations presented are based on the Colebrook-White equation and the accuracy is therefore at best similar.

A recent study of the flow at high Reynolds numbers in smooth pipes [1] showed that the Prandtl law of flow in smooth pipes (Equation 3) was not accurate for high Reynolds numbers. A friction factor correlation of the same form as the Prandtl law was presented (Equation 7).

$$\sqrt{1/f} = 1.889 \log(\text{Re} \sqrt{f}) - 0.358 \quad \text{Equation 7}$$

This correlation differs by as much as 5 % at Reynolds number 3×10^7 compared to Prandtl law of flow in smooth pipes. The Prandtl correlation was shown to predict too low values of the friction factor. Taken into account that the Colebrook-White correlation (Equation 6) is based on the Prandtl law of flow, the same error is to be expected in this correlation at high Reynolds numbers.

FLOW IN ROUGH PIPES

Most pipes cannot be considered ideally smooth at high Reynolds numbers [10]. The investigations of Nikuradse [5] on flow in rough pipes have therefore been of significant interest to engineers. Nikuradse used sand-grains and "Japanese lacquer" to vary the surface roughness of his test pipes. The sand was ordinary building sand, sifted with sieves to get a narrow distribution of sizes. As an example grains of 0.8 mm were obtained by sifting sand with sieves of diameter 0.78 mm and 0.82 mm. In addition "several hundred" sand-grains were measured with a thickness gauge to verify that the arithmetical average was 0.8 mm.

The test pipes in vertical position were filled with thin lacquer, emptied and left to dry for 30 minutes. Then the pipes were filled with sand of a certain size and then emptied. The pipes were then dried for two to three weeks, filled with lacquer again and dried for another two or three weeks. This last layer of lacquer formed a "direct coating" on the wall, and Nikuradse claimed that: "The original form and size of the grains remained unchanged".

In his work Nikuradse used sand-grains and pipes of different diameter to vary the dimensionless parameter r/k_s . According to the theory of dynamic and geometric similarity, the flow behavior should be the same for different choices of pipe diameter and sand-grains, as long the parameter r/k_s was kept constant. Nikuradse's results verified this theory.

Several authors have questioned Nikuradse's measurements. Zagarola [1] gives a critical review of the smooth pipe measurement by Nikuradse [8] (the experimental set-up for Nikuradse's rough pipe experiments was similar to the smooth pipe set-up). Zagarola noted several inconsistencies in Nikuradse's experimental set-up and work. Grigson [11] showed how problems in defining the origin for the logarithmic velocity profile makes it difficult to determine the Von Karman constant from Nikuradse's measurements.

Nevertheless, Nikuradse's sand-grain roughness experiments have been the main reference on flow in rough pipes in over 60 years. In engineering it is common practice [10] to quote the equivalent sand grain roughness as a measure of the hydraulic roughness of a surface or a pipe. In this procedure Equation 4 is used to determine the equivalent sand-grain roughness from measured friction factors. Charts and tables of equivalent sand grain roughness for various materials are given in handbooks, for example [12].

Several authors [13, 14] have investigated turbulent flow in rough pipes with focus on turbulent structure. Raupach et al. [15] reviewed the work on flow over rough walls from various disciplines and showed that there is strong support of the hypothesis of wall similarity. That is, at high Reynolds number the structure of the boundary layer outside the viscous (or roughness) sublayer would have the same structure as a smooth wall boundary layer.

Warburton [16] performed measurements in graphite tubes of different wall roughness. Using compressed air the Reynolds number in the tubes was varied from 3×10^4 to 2.5×10^5 . Warburton used the mean peak-to-valley height measured with a profile meter as a measure of the surface roughness and claimed that the friction factor in graphite tubes might be predicted from direct measurements of surface roughness. However, no information on the tracing length of his roughness measurements was given which makes it difficult to compare his results with the present work.

EXPERIMENTAL WORK

Flow measurements were performed in a high-pressure flow loop fed with natural gas from export pipelines. The natural gas was dry gas with a methane content of approximately 85 % (the molar weight of the gas was typically 18.5 kg/kmol). The gas was kept at constant temperature with heat exchangers, and the rate of flow was measured with sonic nozzles. The flow rate was kept constant by a centrifugal compressor in the loop and the gas composition was measured with a gas chromatograph. Further details are reported by Sletfjerding [7].

Test sections 6 m long with an internal diameter of 150 mm were made of honed steel tubing to ensure high quality tolerance of the inner diameter. The test sections were assembled in the flow loop downstream an 18 m straight section. Upstream the straight section a flow conditioner was placed to ensure fully developed conditions in the test sections.

The pressure drop in the test sections was measured through 4 mm wall taps. For the measurement of differential pressures a high-precision Paroscientific digital differential pressure transducer with an accuracy of 0.01 % of full-scale reading (207 mbar) was used. The absolute pressure and temperature were measured in each test section. Figure 1 shows schematically the design and the instrumentation of the test section.

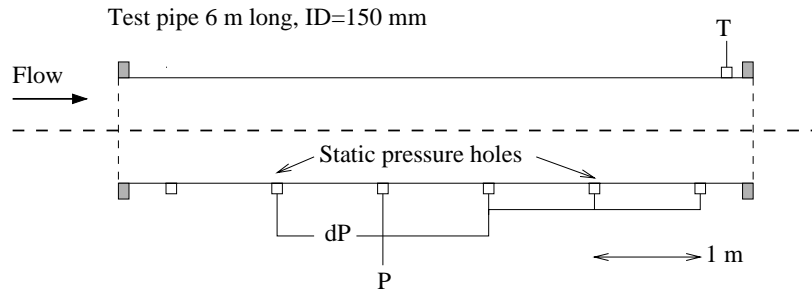


Figure 1: Schematic view of a test pipe

The inside of the 8 test pipes was treated differently. The pipes were coated with a mixture of two component epoxy coating (COPON EP2306 H.F.) and glass beads with different diameter distribution. The sizes and volume concentration of glass beads used in the coating are tabulated in Table 1. Before coating the pipes were sandblasted.

Table 1: Coating of test pipes

Pipe	Coating	Glass-bead size	Volume coating/beads
1	yes	-	-
2	no	-	-
3	yes	0-50 μm	2:1
4	yes	40-70 μm	2:1
5	yes	70-110 μm	2:1
6	yes	90-150 μm	4:1
7	yes	100-200 μm	4:1
8	yes	50-105 μm	2:1

The coating was applied by a high-speed rotating nozzle that was pulled through the pipe at constant speed by a hydraulic winch. The nozzle was fed with coating at constant rate by a membrane pump. During coating all wall taps were plugged to avoid sand and coating to enter the holes. After coating the plugs were removed and the holes were inspected with video equipment and cleaned if necessary. The quality of the coating was also inspected by video equipment and was found to be homogeneous.

ROUGHNESS MEASUREMENTS

The roughness of the inside pipe wall of all pipes was measured with a profilometer (Perthometer SP3) with a stylus radius of 5 μm immediately after the flow tests. The stylus instrument gave as output both roughness parameters (R_a , R_q , R_z) and the measured profile. The output from the stylus instrument was transferred through the external interface to a computer for processing. The roughness profiles were measured at the bottom of the pipe in the axial direction. Figure 2 shows a schematic view of the roughness measurement device.

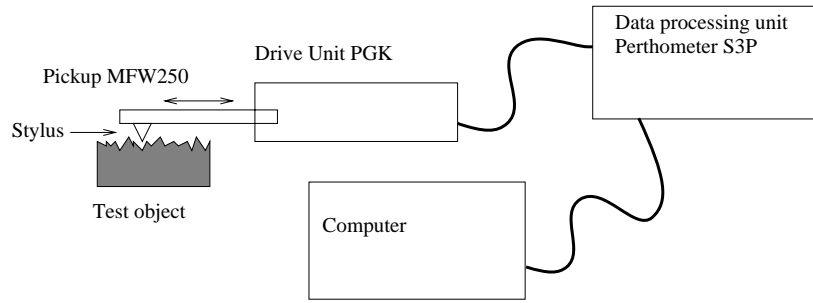


Figure 2: Roughness measurement device

Depending on the roughness of the surface measured, the vertical measuring range of the stylus instrument was chosen to either 25 μm or 250 μm . The instrument digitized the vertical measuring range in 32768 intervals. Therefore the vertical resolution was given by $25\mu\text{m}/16384=1.5 \text{ nm}$ or $250 \mu\text{m}/16384=15 \text{ nm}$ depending on the vertical measuring range chosen. The measuring range 25 μm was used whenever possible.

The cut-off wavelength is the largest wavelength of undulations recorded by the instrument. The cut-off wavelength, λ_c , of the instrument could be chosen to 0.08, 0.25, 0.8 or 2.5 mm. The appropriate cut-off wavelength was chosen according to DIN 4768 [17] depending on the roughness of the surfaces. The total traced length was digitized in 8064 intervals thus the resolution in the horizontal direction was given by $l_t/8064$, where l_t was the total traced length.

RESULTS

The friction factor was calculated from the momentum equation for pipe flow (Equation 1) neglecting the gravity term. Because the pressure drop measurements were made over a short distance (4 m) the flow was assumed to be isothermal at the measured temperature T . The compressibility factor Z was assumed to be constant at an average value (based on the average pressure) over the distance Δx (distance between pressure taps). Using the real gas law $\rho = M_g P / ZRT$, the momentum equation can be rearranged [18]:

$$\frac{M_g}{ZRT} P \Delta P + \frac{1}{2} \frac{\dot{m}^2}{A^2} \frac{f}{D} \Delta x - \frac{\dot{m}^2}{A^2} \frac{\Delta P}{P} = 0 \quad \text{Equation 8}$$

The density and viscosity of the gas in the test section was calculated for each measurement point based on the measured temperature, absolute pressure and gas composition. The gas density (and compressibility factor) was calculated with the AGA-8 correlation [19] and the viscosity with a correlation developed by Chung et al. [20].

Equation 8 was used to calculate the friction factor for each measurement series. The Reynolds number was calculated from the definition:

$$\text{Re} = \frac{\rho \bar{U} D}{\mu} = \frac{4}{\pi} D \frac{\dot{m}}{\mu} \quad \text{Equation 9}$$

Figure 3 (figures 3-10 are found at the end of the paper) shows the measured friction factors versus Reynolds numbers for all 8 test pipes. In the test pipe coated with bare coating two measurement series were done several months apart. The figure shows that the friction factor in the pipes (except the pipe with plain coating) is independent of the Reynolds number, and that the value of the friction factor increases with the increased measured value of the surface roughness. The test pipe coated with plain epoxy coating show smooth pipe flow behavior up to the maximum Reynolds number of 30×10^6 .

Table 2 shows the equivalent sand-grain value for each of the rough pipes. This value was calculated from Equation 4 using the constant value of the measured friction factor for each pipe (this value was taken as the arithmetical mean of the measured friction factors at the four highest Reynolds numbers for each pipe as indicated in Figure 3). No equivalent sand-grain value was calculated for the pipe with plain coating, because the friction factor did not show rough flow characteristics.

Figures 4, 5, 6 and 7 show examples of the measured roughness profiles. The bare steel surface pipe is denoted pipe 2 and the coated pipes 1, 3, 4, 8, 5, 6, 7 according to increasing bead size in the coating (see Table 1). In Figure 4 the coated pipe and the steel pipe are illustrated. The scaling of the axis is equal and the steel pipe appears to have a rougher surface than the coated pipe. In the following three figures (Figures 5, 6 and 7) test pipes 3, 4, 8, 5, 6, 7 are compared with equal scaling on the axis. Figures 5, 6 and 7 show that the roughness of the profiles is increasing according to the increasing bead size in the coating. Note that the axis scaling in these three figures are different from Figure 4.

The measured values of the R_a , R_q , R_z of the test pipes are tabulated in Table 2. The roughness parameters are mean values of 100 samples. Given also is the standard deviation of the measurements and the mean bead size of the glass beads in the coating. The cut-off wavelengths in the measurements were $\lambda_c=0.8$ mm for the pipe coated with plain coating and $\lambda_c=2.5$ mm for the other pipes. In the table the coated pipes are listed according to increasing bead size in the coating. The roughness parameters generally increase with increasing bead size.

Table 2: Roughness of test pipes

Pipe	k_s [μm]	\bar{d}_{bead} [μm]	R_a [μm]	R_q [μm]	R_z [μm]	H [-]
1	-	-	1.08	1.41	6.15	-
2 (steel)	21	-	2.44	3.66	21.28	1.31
3	27	25	4.73	5.98	29.27	1.75
4	62	55	10.65	13.28	62.84	1.47
8	76	78	11.90	14.57	62.66	1.41
5	87	90	16.08	18.82	72.10	1.44
6	142	120	20.95	25.35	98.32	1.32
7	181	150	23.68	31.02	122.10	1.24

The power spectral density (PSD) of all measured profiles was calculated. Figures 8 and 9 show the averages over 100 samples for all eight pipes. The PSD describes how the variance of the measured roughness profile changes with frequency or length scale [21]. The calculation was done using Welch algorithm with a Hanning window in MATLAB (Math Works Inc.).

Several authors [22, 23] have used fractal analysis to characterize rough surfaces and various methods for estimating the fractal dimension of a surface are available [24]. One method is to estimate the so-called Hurst exponent [25] from the PSD function.

$$G(w) \sim w^{-(2H+1)}$$

Equation 10

The PSD function, $G(w)$, scales according to Equation 10, and the Hurst exponent may be calculated by fitting a straight line to the PSD-function in a log-log plot. Table 1 shows the estimated Hurst exponent from the rough test pipes in the study. The Hurst exponent was found to be in the range 1.24 –1.75. For details about the analysis see [7].

For a surface (or signal) to have fractal characteristics the Hurst exponent should be between 0.5 and 1.0 [25]. The surfaces measured in this study did not show fractal scaling. However the calculated exponent was used as a characteristic measure of the slope of the PSD function. The PSD slope measure was combined with the rms-roughness parameter (R_q) to form a roughness measure containing both a height measured and a texture measure.

DISCUSSION

Nikuradse [5] obtained a direct correlation between the diameter of the sand-grains applied on the pipe wall and the measured friction factor. In the present study, the aim was to establish a correlation between the directly measured wall roughness and the friction factor. Figure 10 shows the Nikuradse-type correlation ($\sqrt{1/f} = A \log(r/k) + B$) between the measured roughness parameters and the friction factor. The parameter in the straight line least-square-fit is given in Table 3. For the R_q/H roughness measure, the maximum deviation between the measured friction factor and the least square fitted correlation was 1.6 %. The uncertainty in the measured friction factor was ± 2.8 % [7]

Table 3: Constants in the curve fit of $(1/f)^{1/2}$ versus $\log(r/k)$

Roughness parameter	A	B
R_a	1.90	0.51
R_q	2.06	0.10
R_z	2.53	-0.04
R_q/H'	1.94	0.26
k_s (Nikuradse)	2.00	1.74

The results show that by combining a height measure (R_q) of the wall roughness and a texture parameter (H), an improved fit (compared to standard roughness measured) is obtained between the measured friction factor and the wall roughness in rough pipe flow. In developing more accurate ways of estimating pressure drop due to wall roughness in pipeline flow both the height of protrusions on the pipe wall and their spatial distribution should be taken into account. Our results enable calculation of pipeline pressure drop and pipeline capacity from direct measurements of wall roughness using one height and one texture parameter. The results make it possible progress further towards understanding the interaction between wall roughness and pressure drop in pipelines.

CONCLUSIONS

The results from flow experiments at high Reynolds numbers in roughened pipes showed that the friction factor was independent of Reynolds number when wall roughness was large.

A combination of the root-mean-square roughness and the slope of the power spectrum of the measured roughness profile were found to correlate well with measured friction factors.

A new correlation between the directly measured wall roughness and the friction factor valid in rough flow was proposed.

The results showed that turbulent flow at high Reynolds number are very sensitive to small changes in surface roughness

ACKNOWLEDGEMENTS

Flow experiments were performed at the Kårstø Metering and Technology Laboratory (K-Lab), a Statoil operated research and calibration laboratory. The research was sponsored by Statoil.

NOMENCLATURE

A =	Pipe cross-sectional area, m ²
D =	Pipe diameter, m
f =	Friction factor (Moody)
G =	Power spectral density (PSD)
H =	Hurst exponent
k _s =	Sand-grain roughness, m
l _t =	Tracing length, m
M _g =	Gas mole weight, kg/kmol
P =	Pressure, Pa
ΔP =	Pressure drop, Pa
R =	Universal gas constant, J/kmol K
Re =	Reynolds number, $Re = \rho \bar{U} D / \mu = w D / \mu A$
R _a =	Arithmetic mean roughness, m
R _q =	Root mean square roughness, m
R _z =	Mean peak-to-valley height, m
T =	Temperature, K
U =	Mean velocity, m/s
m =	Mass flow rate, kg/s
x =	Axial coordinate, m
Δx =	Distance between pressure taps, m
Z =	Compressibility factor
ρ =	Gas density, kg/m ³
w =	Radial frequency, 1/m
μ =	Dynamic viscosity, Pa s
λ _c =	Cut-off wavelength, m
¯ =	Superscript, mean value

REFERENCES

1. Zagarola, M.V. (1996): Mean-flow scaling of turbulent pipe flow, Ph.D. thesis, Princeton University, USA.
2. Barenblatt, G.; Chorin, A. and Prostokishin, P. (1997): Scaling laws for fully developed turbulent flow in pipes, *Applied Mechanics Review*, **50**(7) p 413-429.
3. Colebrook, C. (1939): Turbulent flow in pipes, with particular reference to the transition regime between smooth and rough pipe laws, *Institution of Civ. Eng. Journal*, **11**, p133-156.
4. Grigson, C. (1992): Drag losses of new ships caused by hull finish, *Journal of Ship Research*, **36**(2), p182-196.
5. Nikuradse, J. (1933): Stromungsgesetze in rauhen rohren, In *Forschungsheft 361*, Volume B, VDI Verlag, Berlin (Jul./Aug).
6. Patel, V.C. (1998): Perspective: Flow at high Reynolds numbers and over rough surfaces - Achilles heel of CFD, *Journal of Fluids Engineering*, **120** p434-444.
7. Sletfjerding, Elling (1999): Friction factor in smooth and rough gas pipelines, Doktor Ingeniør Thesis, Norwegian University of Science and Technology, Trondheim, Norway.
8. Nikuradse, J. (1966): Gesetzmässigkeiten der turbulenten stromung in glatten rohren, In *Forschungsheft 356*, volume B. VDI Verlag Berlin (1932). Translated in NASA TT F-10, 359.
9. Haaland, S. (1983): Simple and explicit formulas for the friction factor in turbulent pipe flow" *Journal of Fluids Engineering*, **105**, p89-90.
10. Schlichting, H. (1979): *Boundary layer theory* (Seventh Edition). McGraw-Hill Inc., New York. Translated by Dr. J. Kestin.
11. Grigson, C. (1984): Nikuradse's experiment, *AIAA Journal*, **22**(7) p999-1001
12. Blevins, R.D. (1992): *Applied Fluid Dynamics Handbook*. Krieger Publishing Company, Florida, USA.
13. Robertson, J., Martin, J., and Burkhart, T. (1968): Turbulent flow in rough pipes. *I and EC Fundamentals*, 7(2):253--265..
14. Powe, R. and Townes, H.: Turbulent structure in rough pipes. *Journal of Fluids Engineering*, pages 255-262. (1973).
15. Raupach, M., Antonia, R., and Rajagopalan, S.: Rough wall turbulent boundary layers. *Appl. Mech. Rev.*, 44(1) (1991).
16. Warburton, C. (1974): Surface roughness of graphite and its effect on friction factor. *Proc. Instn. Mech. Engrs*, 188(457-460).
17. Sander, M. (1991): *A Practical Guide to the Assessment of Surface Texture*. Feinpruf GmbH, Göttingen Germany.
18. Smith, R., Miller, J., and Ferguson, J. (1956): Flow of natural gas through experimental pipelines and transmission lines, Bureau of Mines, Monograph 9, American Gas Association.
19. Starling, K. E. (1992): Compressibility factors of natural gas and other related hydrocarbon gases, Transmission Measurement Committee Report no. 8, American Gas Association.
20. Chung, T., Ajlan, M., Lee, L. and Starling, K. (1988): Generalized multi-parameter correlation for nonpolar and polar fluid transport properties, *Industrial and Chemical Engineering Research*, **27**, p671-679.
21. Bendat, J. and Piersol, A. (1986): *Random Data, Analysis and Measurement Procedures*, John Wiley and Sons, New York.
22. Ganti, S. and Bhushan, B. (1995): Generalized fractal analysis and its application to engineering surfaces, *Wear*, **180**, pp. 17-34.
23. Sayles, R. and Thomas, T. (1978): Surface topography as a nonstationary random process, *Nature*, **271** pp. 431-434.
24. Schmittbuhl, J., Vilotte, J.-P., and Roux, S. (1995): Reliability of self-affine measurements, *Physical Review E*, **51**(1), pp. 131-147.
25. Feder, J. (1988): *Fractals*, Plenum Publishing Company, New York.

FIGURES

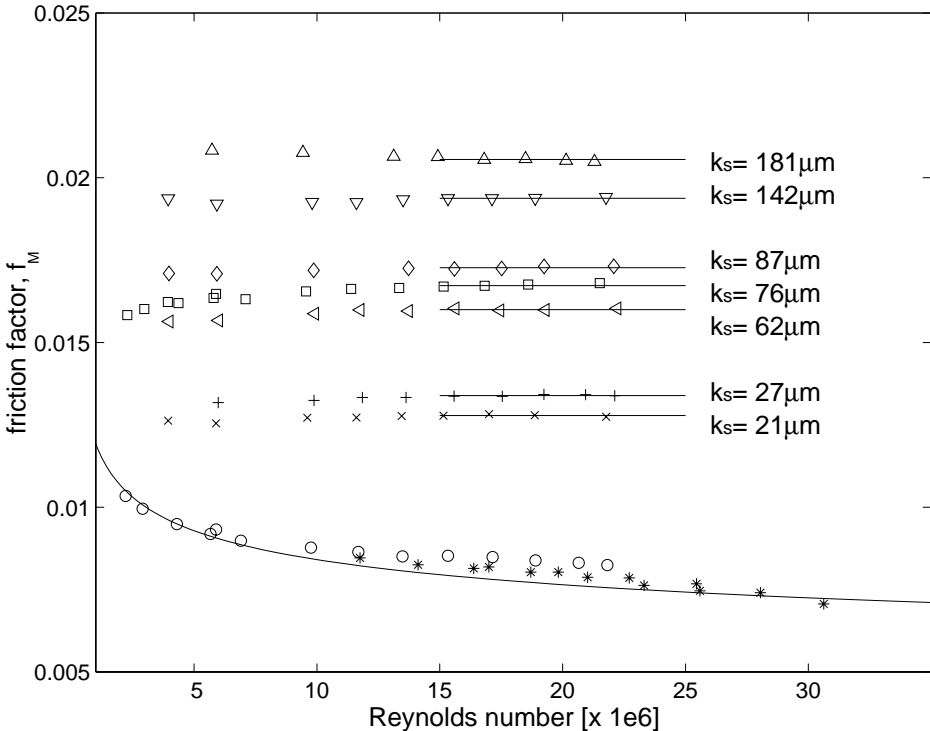


Figure 3: Measured friction factor in test pipes: o: coated pipe (series 1), *: coated pipe (series 2) x: steel pipe, +: pipe 3, <: pipe 4, □: pipe 8, ◇: pipe 5, ∇: pipe 6, △: pipe 7, line: Zagarola friction factor

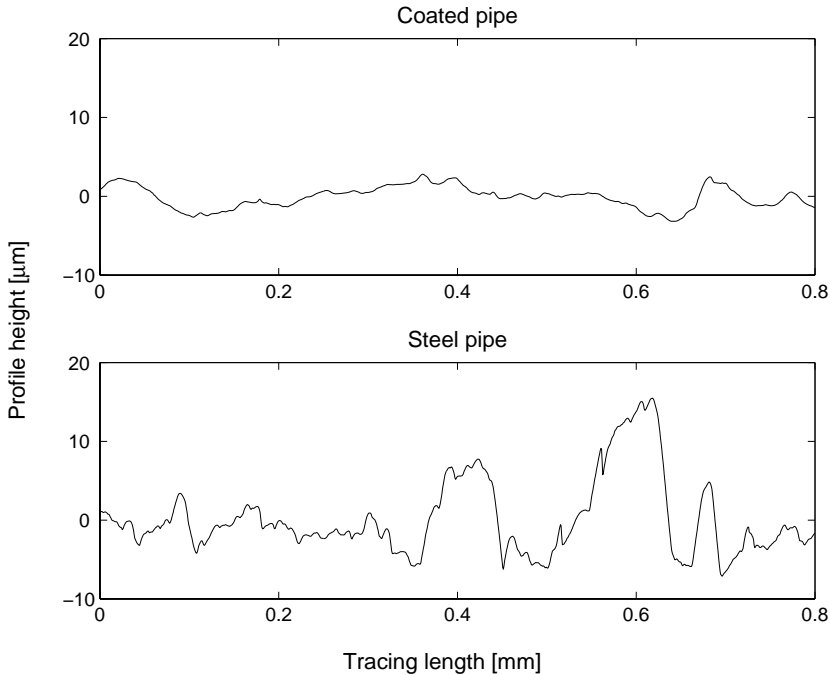


Figure 4: Measured roughness profiles pipe 1 and 2.

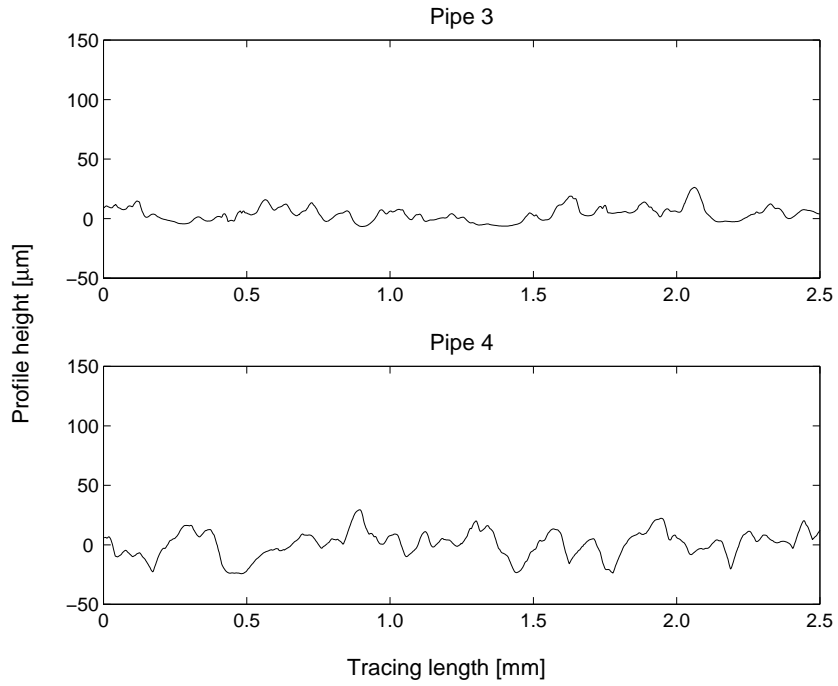


Figure 5: Measured roughness profile pipe 3 and 4.

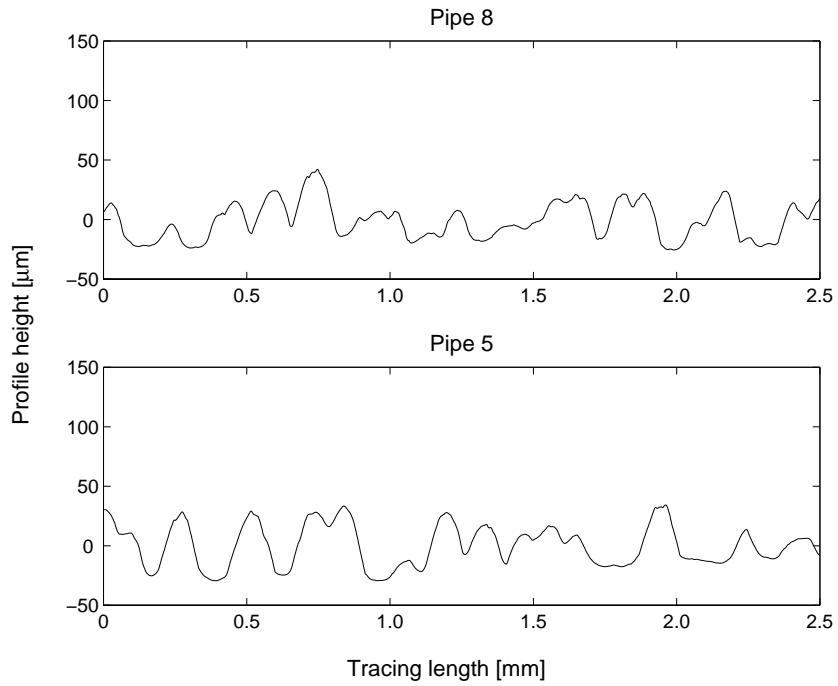


Figure 6: Measured roughness profile pipe 8 and 5.

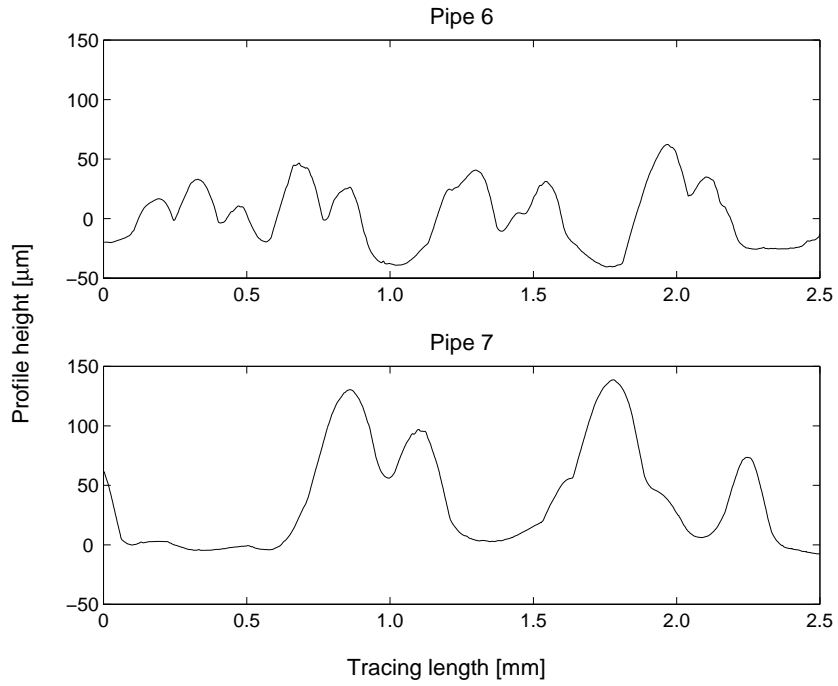


Figure 7: Measured roughness profile pipe 6 and 7.

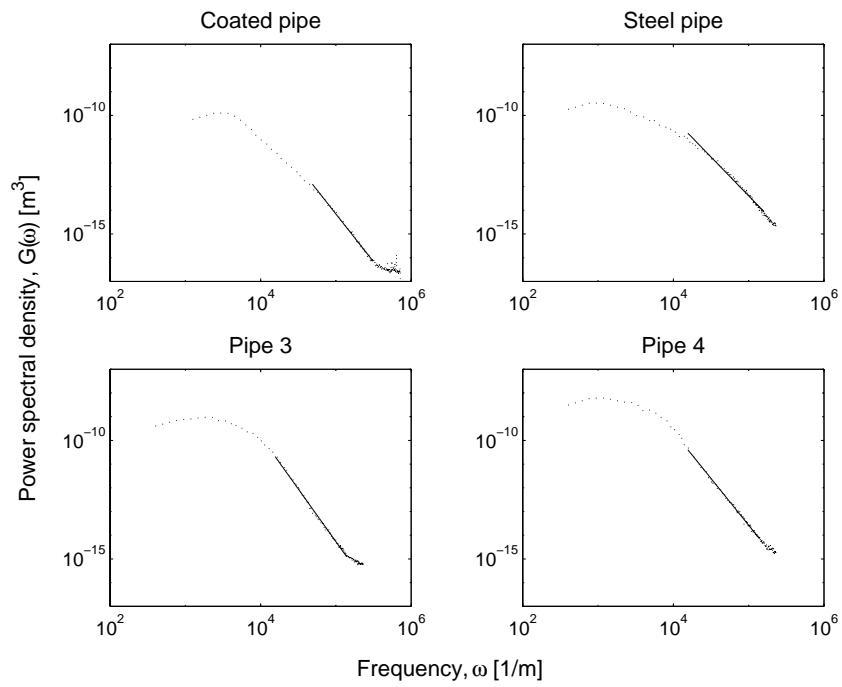


Figure 8: Power spectral density of measured wall roughness pipe 1-4

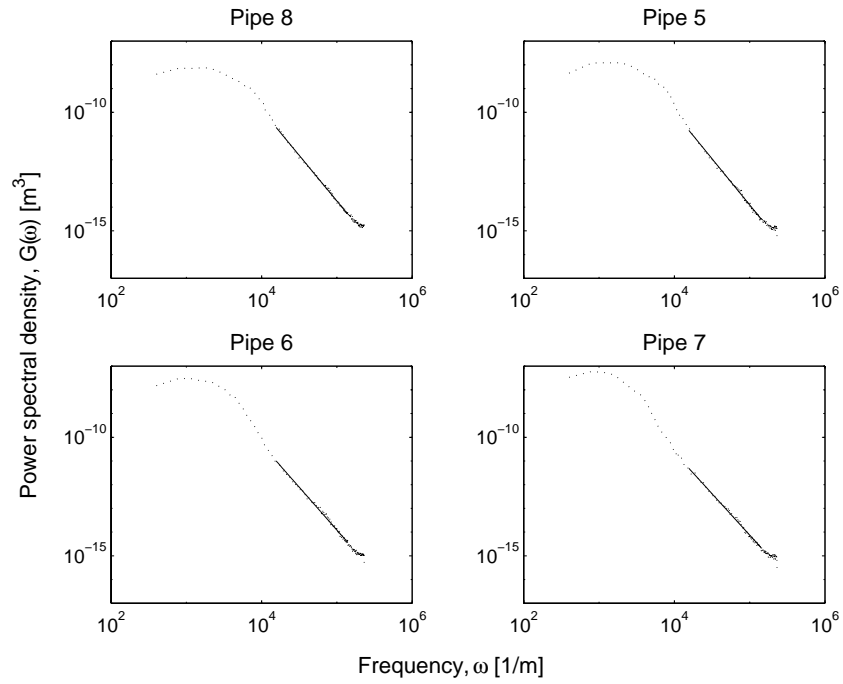


Figure 9: Power spectral density of measured wall roughness pipe 5-8

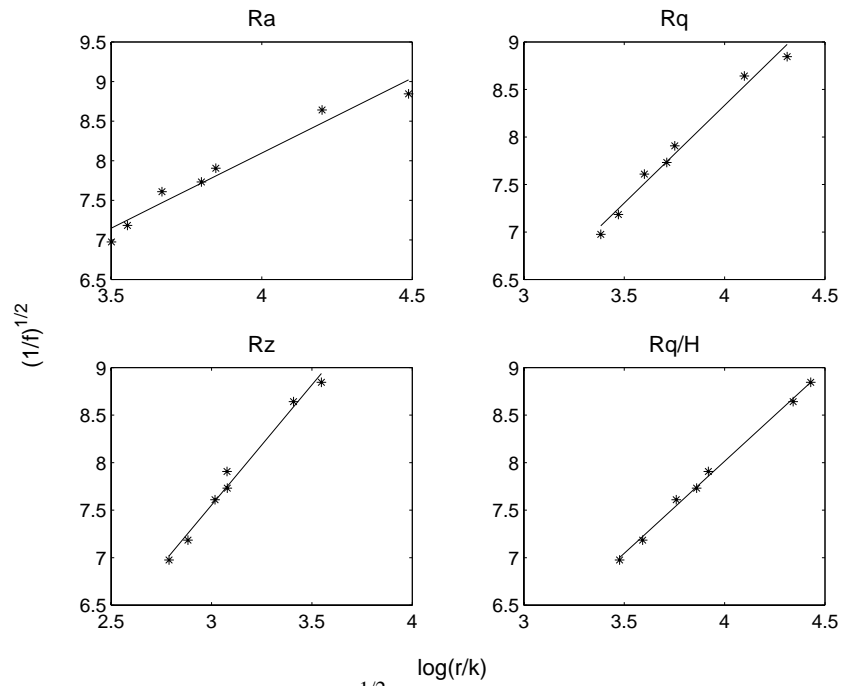


Figure 10: Correlations between $(1/f)^{1/2}$ and $\log(r/k)$ for the different roughness measures